

University of Groningen

Large yield production of high mobility freely suspended graphene electronic devices on a polydimethylglutarimide based organic polymer

Tombros, Nikolaos; Veligura, Alina; Junesch, Juliane; van den Berg, J. Jasper ; Zomer, Paul J.; Wojtaszek, Magdalena; Vera Marun, Ivan J.; Jonkman, Harry T.; Wees, Bart J. van

Published in:
Journal of Applied Physics

DOI:
[10.1063/1.3579997](https://doi.org/10.1063/1.3579997)

IMPORTANT NOTE: You are advised to consult the publisher's version (publisher's PDF) if you wish to cite from it. Please check the document version below.

Document Version
Publisher's PDF, also known as Version of record

Publication date:
2011

[Link to publication in University of Groningen/UMCG research database](#)

Citation for published version (APA):

Tombros, N., Veligura, A., Junesch, J., van den Berg, J. J., Zomer, P. J., Wojtaszek, M., ... Wees, B. J. V. (2011). Large yield production of high mobility freely suspended graphene electronic devices on a polydimethylglutarimide based organic polymer. *Journal of Applied Physics*, 109(9), 093702-1-093702-5. [093702]. <https://doi.org/10.1063/1.3579997>

Copyright

Other than for strictly personal use, it is not permitted to download or to forward/distribute the text or part of it without the consent of the author(s) and/or copyright holder(s), unless the work is under an open content license (like Creative Commons).

Take-down policy

If you believe that this document breaches copyright please contact us providing details, and we will remove access to the work immediately and investigate your claim.

Downloaded from the University of Groningen/UMCG research database (Pure): <http://www.rug.nl/research/portal>. For technical reasons the number of authors shown on this cover page is limited to 10 maximum.

Large yield production of high mobility freely suspended graphene electronic devices on a polydimethylglutarimide based organic polymer

Nikolaos Tombros, Alina Veligura, Juliane Junesch, J. Jasper van den Berg, Paul J. Zomer, Magdalena Wojtaszek, Ivan J. Vera Marun, Harry T. Jonkman, and Bart J. van Wees

Citation: *Journal of Applied Physics* **109**, 093702 (2011); doi: 10.1063/1.3579997

View online: <https://doi.org/10.1063/1.3579997>

View Table of Contents: <http://aip.scitation.org/toc/jap/109/9>

Published by the [American Institute of Physics](#)

Articles you may be interested in

[A transfer technique for high mobility graphene devices on commercially available hexagonal boron nitride](#)
Applied Physics Letters **99**, 232104 (2011); 10.1063/1.3665405

[Fast pick up technique for high quality heterostructures of bilayer graphene and hexagonal boron nitride](#)
Applied Physics Letters **105**, 013101 (2014); 10.1063/1.4886096

[A ballistic pn junction in suspended graphene with split bottom gates](#)
Applied Physics Letters **102**, 223102 (2013); 10.1063/1.4807888

[Making graphene visible](#)
Applied Physics Letters **91**, 063124 (2007); 10.1063/1.2768624

[Current-induced cleaning of graphene](#)
Applied Physics Letters **91**, 163513 (2007); 10.1063/1.2789673

[Realization of a high mobility dual-gated graphene field-effect transistor with Al₂O₃ dielectric](#)
Applied Physics Letters **94**, 062107 (2009); 10.1063/1.3077021

AIP | Journal of
Applied Physics

SPECIAL TOPICS



Large yield production of high mobility freely suspended graphene electronic devices on a polydimethylglutarimide based organic polymer

Nikolaos Tombros,^{1,2,a)} Alina Veligura,² Juliane Junesch,² J. Jasper van den Berg,² Paul J. Zomer,² Magdalena Wojtaszek,² Ivan J. Vera Marun,² Harry T. Jonkman,¹ and Bart J. van Wees²

¹Molecular Electronics, Zernike Institute for Advanced Materials, University of Groningen, The Netherlands

²Physics of Nanodevices, Zernike Institute for Advanced Materials, University of Groningen, The Netherlands

(Received 11 November 2010; accepted 17 February 2011; published online 2 May 2011)

The recent observation of a fractional quantum Hall effect in high mobility suspended graphene devices introduced a new direction in graphene physics, the field of electron–electron interaction dynamics. However, the technique used currently for the fabrication of such high mobility devices has several drawbacks. The most important is that the contact materials available for electronic devices are limited to only a few metals (Au, Pd, Pt, Cr, and Nb) because only those are not attacked by the reactive acid etching fabrication step. Here we show a new technique that leads to mechanically stable suspended high mobility graphene devices and is compatible with almost any type of contact material. The graphene devices prepared on a polydimethylglutarimide based organic resist show mobilities as high as $600.000 \text{ cm}^2/\text{Vs}$ at an electron carrier density of $n = 5.0 \times 10^9 \text{ cm}^{-2}$ at 77 K. This technique paves the way toward complex suspended graphene based spintronic, superconducting, and other types of devices. © 2011 American Institute of Physics. [doi:10.1063/1.3579997]

I. INTRODUCTION

The widely accepted method to produce a suspended graphene electronic device is to deposit graphene on a silicon oxide (SiO_2) coated Si substrate,^{1,2} connect the graphene layer to Cr/Au electrodes, and remove a part of the SiO_2 using wet etching with buffered hydrofluoric acid (BHF).^{3–7} This technique has some serious drawbacks, however. Because this etching is isotropic, the SiO_2 below the narrow Cr/Au contacts is also partially removed,^{3–7} which can lead to mechanically unstable devices and a low yield of working devices. In addition, the contact materials available for electronic devices are limited to Au, Pd, Pt, Cr, and Nb, because only those five metals are not attacked by BHF etching.⁸ All other materials—metals (Al, Ti, Cu, etc.), oxides (Al_xO_y , MgO, indium tin oxide, etc.), ferromagnets (Co, Ni, Py, etc.), half metals (CrO_2 , $\text{La}_{(1-x)}\text{Sr}_x\text{MnO}_3$, etc.) and other anorganic materials necessary for the fabrication of graphene based spintronic,⁹ superconducting,¹⁰ optoelectronic, and other types of devices—are etched by BHF. Therefore, it is crucial to find a method to produce a suspended graphene device that excludes this aggressive BHF etching step.

II. EXPERIMENT

In this paper, we present a unique technique that circumvents the above-stated limitations and leads to very mechanically stable suspended graphene devices with a remarkably high yield. The idea is to deposit graphene on an organic polymer and to remove the polymer underneath the graphene layer in a controllable way using an organic solvent that is

harmless to anorganic materials such as metals, insulators, and ferromagnets (Fig. 1). Multilayer resist technologies have previously been used for the fabrication of suspended

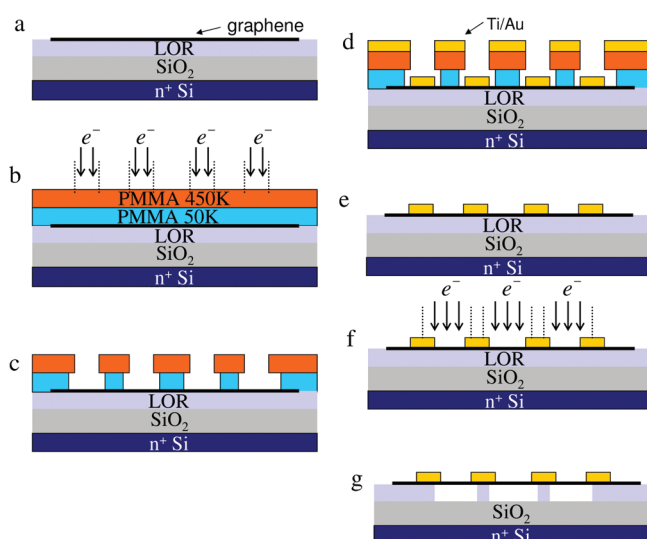


FIG. 1. (Color online) Fabrication procedure of a suspended graphene device on a LOR. (a) The Scotch tape technique is used to deposit graphene on a LOR layer. (b) For the electron beam lithography (EBL) step, we spin coat two polymethylmethacrylate (PMMA) polymer resists on top of the graphene layer, the low molecular weight resist PMMA 50 K and the high molecular weight resist PMMA 450 K. Exposure is done at 30 keV with an area dose of $180 \mu\text{C}/\text{cm}^2$. (c) Development of the exposed areas is done using xylene at 21°C . The undercut obtained in the EBL exposed structures is necessary for successful lift-off. (d) Evaporation of Ti/Au. (e) Lift-off is done in hot xylene ($T = 80^\circ\text{C}$). (f) The parts of the graphene layer that should be suspended are exposed with the EBL at 30 keV and area dose $1050 \mu\text{C}/\text{cm}^2$. Note that instead of an EBL step, deep-UV exposure also can be used to expose the LOR [see Fig. 4(b)]. (g) Suspended graphene is obtained after removal of the exposed LOR with ethylacetate developer at 21°C .

^{a)}Author to whom correspondence should be addressed. Electronic mail: n.tombros@rug.nl.

carbon nanotube devices;^{11,12} however, those cannot be used for the production of mechanically stable large size suspended graphene devices or with complex structures such as suspended top gates and graphene patterned by etching. We used LOR-A (MicroChem), a polydimethylglutarimide (PMGI) based organic lift-off resist (LOR) that shows excellent resistance to a wide range of solvents and is stable at temperatures up to 190 °C. As we show later in the paper, this technique is compatible not only with plasma etching techniques that can be used, for example, to etch a well-defined Hall bar structure in graphene, but also with techniques for the production of free-standing top gates in order to obtain electrostatically defined free-standing bilayer graphene quantum dots and graphene pn junctions. This technique can also be used to produce a suspended graphene device on a flexible substrate for the investigation of mechanical strain related effects on the mobility and bandgap of bilayer and single layer graphene.

The devices were prepared as shown in Fig. 1 (see Sec. V). Highly n-doped (0.007 Ωcm) 4 inch Si wafers covered with a 300 nm (or 500 nm) silicon oxide dielectric were used as a starting material, onto which we spin coated a layer of LOR-A polymer 1.15 μm in thickness. This thickness provides good graphene visibility in the green spectrum when using an optical microscope. We deposited highly oriented pyrolytic graphite (HOPG) graphene onto the LOR-A polymer using the Scotch tape technique² [Fig. 1(a)]. Standard electron beam lithography (EBL) was used to fabricate a graphene electronic device [Figs. 1(b) and 1(c)]. We evaporated 5 nm of Ti as an adhesion layer and 75 nm of Au using an e-gun evaporator at a pressure of 4.0×10^{-7} mbar [Fig. 1(d)]. A crucial step is lift-off [Fig. 1(e)], which is done in hot xylene (80 °C), an organic solvent that at this temperature is active enough to dissolve the PMMA layers but which does not at all affect the (EBL exposed) LOR. To make the graphene suspended, a second EBL step is used to expose the LOR underneath the graphene layer [Figs. 1(f) and 1(g)]. We developed in ethyl lactate to remove the EBL exposed LOR, rinsed the sample in hexane, and gently blew it dry with nitrogen.

III. RESULTS AND DISCUSSION

All of the suspended graphene devices we have made so far (26 in total) with lateral sizes up to 10 μm have remained intact after this procedure, and this, remarkably, is without the use of a critical point drying system. There are three reasons for this. First, the surface tension of hexane, $\gamma = 18$ nN/μm, is far too weak to rupture the suspended graphene layer during the drying process. The capillary force F_c that the solvent applies on a suspended graphene membrane with a width W and length L that is suspended at a distance d away from the substrate is $F_c = 2W(L + d)/d\gamma\cos\theta$.¹³ Because hexane, the suspended graphene layer, and any possible PMMA/LOR polymer contaminants on it are all hydrophobic, the wetting is very good, resulting in a contact angle of $\sim 0^\circ$. The capillary force applied on a suspended graphene layer with $L = 10$ μm and $W = 1$ μm is in this case around $F_{c0} = 0.4$ μN; however, the total (uniaxial) force needed to

break a graphene layer with a width of 1 μm is approximately 42 μN,¹⁴ which is more than 2 orders of magnitude larger. Second, given that the distance between the suspended graphene and the SiO₂ substrate is 1.15 μm, the chance that the graphene layer will stick to the SiO₂ surface via the van der Waals force is small, as the graphene layer would first have to be stretched by $\varepsilon \sim 3\%$ in order to reach the substrate. Taking into account that the elastic constant E of graphene¹⁴ is ~ 340 N/m, a strain of $\varepsilon = 3\%$ requires a capillary force of $F_c = 2dWE\varepsilon/L = 2.2$ μN $\gg F_{c0}$. And third, each of the metallic electrodes connected to the graphene layer is supported by a solid pillar of LOR polymer [Fig. 1(g)], which makes the suspended graphene device very mechanically stable, not only against surface tension but also with regard to the electrostatic force applied during gate voltage measurements. This last property is what is lacking in large size suspended graphene devices produced by BHF etching of the SiO₂ substrate, in which the parts of the metallic electrodes on top of the graphene layer are not supported anymore by solid pillars of SiO₂ and can therefore become very mechanically unstable.³⁻⁷

Characterization of the electronic quality of the suspended graphene devices was performed using a standard lock-in technique by sending a current of 10 nA up to 1 μA through the device in two-probe and four-probe geometries. All of our suspended devices show very low ohmic contact resistance (< 60 Ω) between the Ti/Au contacts and the graphene, which is important for metrology purposes in order to obtain an accuracy of 1 ppm or higher in the quantum resistance standard. Our suspended devices usually show strong p-doping, and current annealing¹⁵ is needed to remove the dopants originating from the PMMA and LOR polymer remains that cover the suspended graphene layer. The device shown in Figs. 2(a) and 2(b) (device A) was originally designed to test whether it is possible to create a 10 μm suspended graphene layer without the use of a critical point drying system. Each part of the graphene layer between the Ti/Au electrodes was shown to be suspended after inspection under a scanning electron microscope. The graphene layer is suspended 1.15 μm above the 500 nm thick SiO₂ layer and has a gate capacitance of 10.5 aF/μm² (see below). The majority of the suspended regions shows strong p-doping, except for one area [Fig. 2(c)] showing very low doping, for which we extracted at $T = 77$ K a mobility of 37,000 cm²/Vs at a hole charge carrier density of $n_h = 4.7 \times 10^{10}$ cm⁻² [Fig. 2(d)]. Current annealing (250 μA dc current) of the 4 μm long suspended part of the graphene device at $T = 77$ K resulted in a 600,000 cm²/Vs mobility device at an electron charge carrier density of $n_e = 5.0 \times 10^9$ cm⁻². Note that at this specific carrier density the first derivative of the resistivity curve versus gate voltage shows a maximum, which we interpret as the crossover into the metallic electron regime, where we can extract a well-defined mobility.

The suspended graphene device shown in Fig. 3(a) (device B) has a slightly lower capacitance of 8.6 aF/μm², because it was prepared on a SiO₂ insulating layer 300 nm in thickness and coated with a LOR-A resist 1.4 μm in thickness. This capacitance is extracted from the two-probe quantum Hall measurements in Fig. 3(d). Note that the

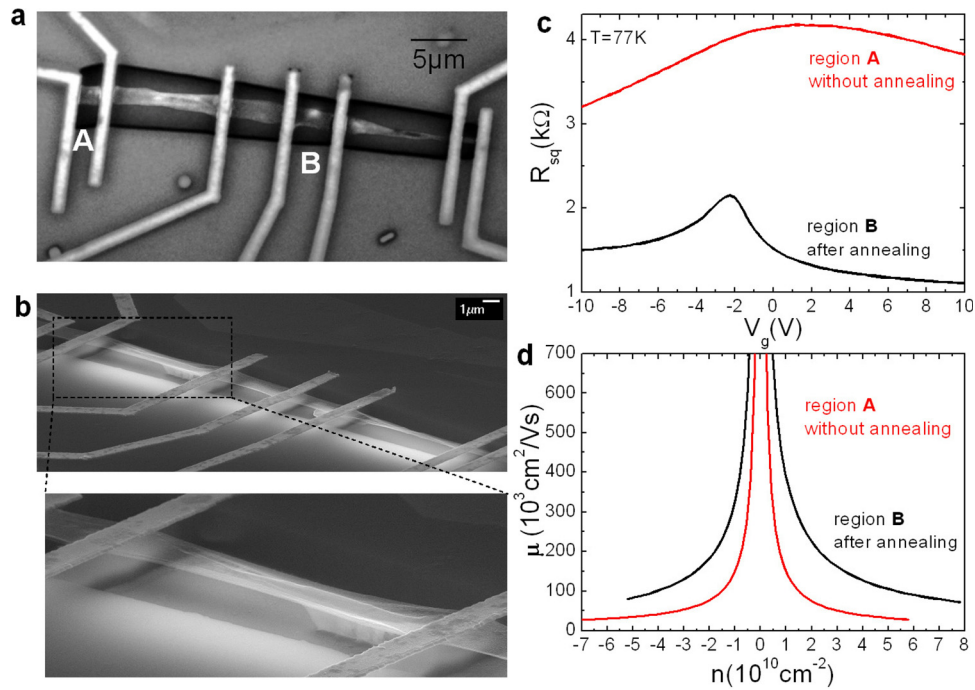


FIG. 2. (Color online) Suspended graphene device on a LOR polymer layer. (a) Optical image of a 40 μm long graphene layer with 80 nm thick Ti/Au electrodes and suspended graphene parts of (from left to right) 2, 10, 5, 4, 10, and 2 μm . (b) Picture taken with a scanning electron microscope under an angle of 70° . A zoomed view of the 10 μm long suspended graphene layer shows a small amount of LOR-A resist underneath the graphene layer that was not removed completely after 1 min of development in ethylacetate. This issue can be resolved by increasing the development time from 1 min (used for this device) to 1.5 to 2 min. The dissolution rate of the LOR layers is around 1.5 $\mu\text{m}/\text{min}$ when exposed with 30 keV electrons at an area dose of 1050 $\mu\text{C}/\text{cm}^2$. (c) The resistivity of the 2 μm long suspended graphene part (region A) shown already before a current annealing step; there is a clear Dirac neutrality point at $V_g = 1$ V applied gate voltage. All other suspended graphene regions show strong p-doping, and a current annealing step is needed to clean up the polymer remains from the suspended graphene in order to observe the Dirac neutrality point at ~ 0 V gate voltage. (d) The mobility of the suspended graphene layer in region A is around 37.000 cm^2/Vs at $n_h = 4.7 \times 10^{10} \text{cm}^{-2}$, for which no current annealing was used. Region B shows a mobility of 600.000 cm^2/Vs at $n_e = 5.0 \times 10^9 \text{cm}^{-2}$ after current annealing.

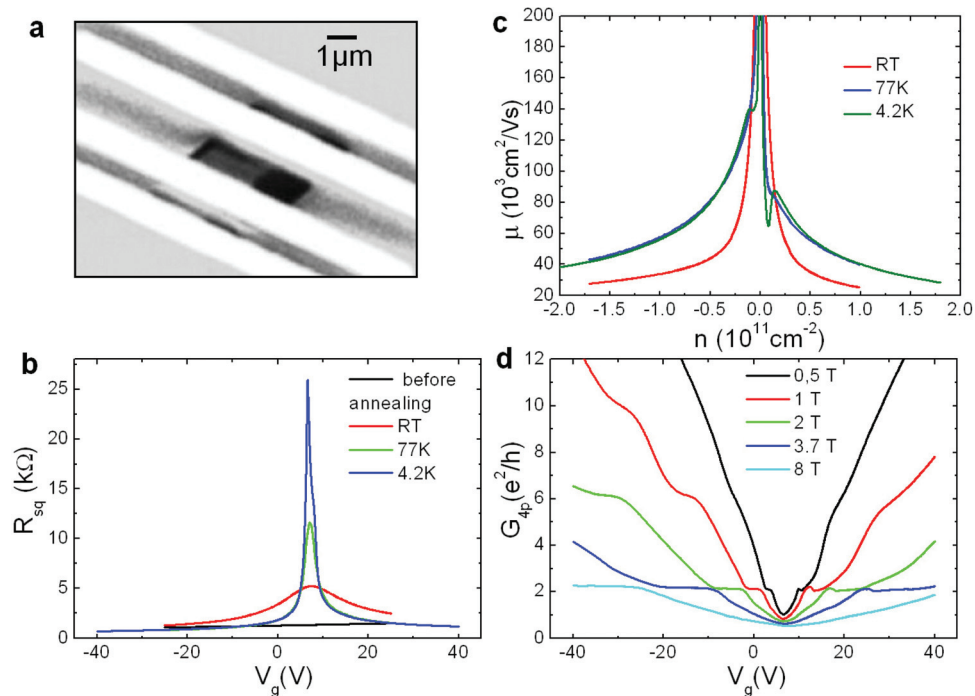


FIG. 3. (Color online) Electronic measurements on a suspended graphene device prepared on a 1.4 μm thick LOR (300 nm thick SiO_2). (a) Optical image of the sample. The outer Au electrodes are connected to a current source, and the inner electrodes are connected to a voltage probe. (b) The device was initially heavily p-doped, and after current annealing at room temperature (RT) in vacuum (10^{-5} mbar) we obtained a clear Dirac neutrality point at $V_g \sim 8$ V. The Dirac linewidth becomes very narrow at 77 K. The resistivity increases by a factor of 5 from RT to 4.2 K. (c) The RT mobility at $n_h = 2.2 \times 10^{10} \text{cm}^{-2}$ is 70.000 cm^2/Vs and increases to 250.000 cm^2/Vs at 77 K and $n_h = 1.0 \times 10^9 \text{cm}^{-2}$. (d) Application of an external magnetic field \mathbf{B} perpendicular to the suspended graphene layer at 4.2 K. The characteristic quantum resistance plateaus for graphene at $2G_0$, $6G_0$, and $10G_0$ are clearly visible at a magnetic field of 1 T. The $2G_0$ plateau is already well developed at $\mathbf{B} = 0.5$ T, which is a clear indication of the excellent electronic quality of our suspended graphene device.

geometrical capacitance for this device is 30% smaller than the one extracted from the quantum Hall filling factors. All mobilities presented in this work are therefore calculated using the electrically measured capacitance. Note that a similar discrepancy on the order of 15% to 30% between the geometrical and electrically defined capacitances was also found in other experimental studies.^{1,5} On this device, we performed a current annealing step in vacuum (10^{-5} mbar) at room temperature (290 K) by sending a 400 μ A dc current through the 3.2 μ m wide suspended graphene, which resulted in a slightly p-doped device with a mobility of 70,000 cm^2/Vs at $n_h = 2.2 \times 10^{10} \text{ cm}^{-2}$ [Figs. 3(b) and 3(c)]. At $T = 77$ K, the mobility increased to 250,000 cm^2/Vs ($n_h = 1.0 \times 10^9 \text{ cm}^{-2}$). In Fig. 3(d), we present the conductance of the device under a magnetic field applied perpendicular to the graphene layer at temperature $T = 4.2$ K. The appearance of the Landau plateau with the filling factor $\nu = 2$ at a magnetic field of only 0.5 T is a clear indication of the excellent electrical quality of the graphene layer. This, together with the linear dependence of filling factors 2, 6, and 10 on the gate voltage, implies that possible sagging and/or deformation (e.g., due to electrostatic force from the gate electrode) is not important.³

We note that both devices presented in this paper, although exposed to 30 keV electrons during the EBL exposure, still show excellent conducting properties and high mobility, indicating that a 30 keV low dose exposure does not introduce any significant damage to the graphene crystal. Note that we cannot exclude some (amorphous) carbon deposition due to the electron beam exposure of the uncovered graphene. Because we can obtain equally high mobilities using current annealing as with processes that do not require electron beam exposure, we conclude that any deposited carbon, if already present, does not limit the electronic quality. We have also performed measurements on a suspended graphene device with four electrodes in a Hall geometry, wherein we find a mobility of 380,000 cm^2/Vs ($n_e = 2.5 \times 10^9 \text{ cm}^{-2}$, $T = 4.2$ K), showing behavior similar to that of sample B. We have also succeeded in obtaining suspended graphene devices etched into a Hall bar geometry using a pure oxygen plasma in a reactive ion etching system [Fig. 4(a)].¹⁶ Such types of devices will be used for a more precise investigation of electron–electron interactions in graphene. Because the PMGI based resist is sensitive to deep-UV light, standard optical lithography can be used for the large scale preparation of suspended graphene devices [Fig. 4(b)].¹⁶

IV. CONCLUSIONS

In conclusion, we present a technique for the production of a suspended graphene device on a PMGI based resist that shows superior behavior as compared to the fabrication technique used currently by the graphene community, in which a suspended graphene device is obtained after BHF etching of the SiO_2 substrate. First, the technique is compatible with all anorganic contact materials such as metals, ferromagnets, and insulators, which is not the case for the BHF etching technique, with which only five contact materials—Au, Pd, Pt, Cr, and Nb—are inert to the strong acid. Second, as long

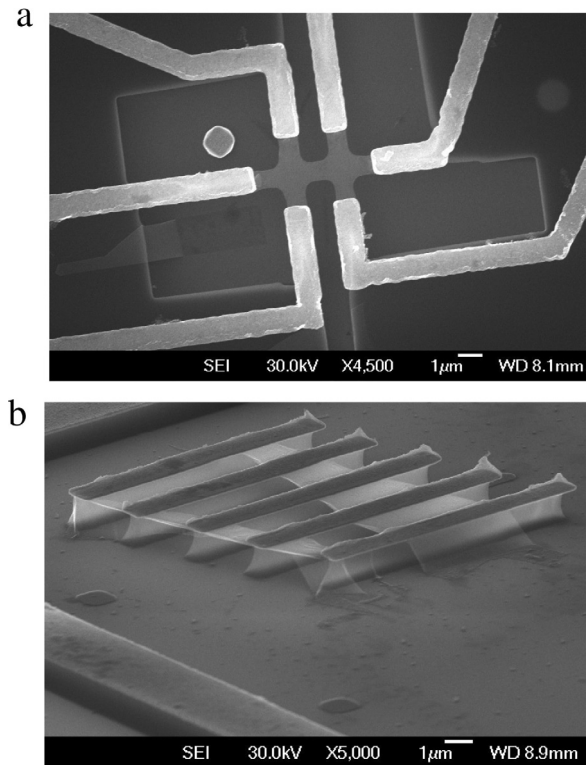


FIG. 4. Scanning electron microscope pictures showing the potential of the new technique. (a) Top view of a freely suspended graphene Hall bar at a distance of 1.15 μ m from the SiO_2 substrate. We introduced two extra fabrication steps in between steps e and f (Fig. 1) in order to etch a Hall bar (see Sec. V). (b) Side view under a 70° angle. Here, instead of the final EBL exposure, we introduced a short deep-UV exposure followed by development in ethyllactate in order to obtain suspended graphene (step f, Fig. 1). Note that the LOR below the gold contacts is not exposed, because the 75 nm thick gold functions as a mask layer for the deep-UV light. This shows the potential of using optical lithography for the mass production of suspended graphene devices fabricated with this technique.

as the distance between the suspended graphene and the substrate is large enough, this technique does not require the use of a critical point drying system, an instrument that is a necessary tool for the production of suspended graphene devices 2 μ m or longer when the BHF method is used.^{3–7} And third, mechanical stability is ensured in the LOR-A suspended devices because each of the electric contacts affixed to the suspended graphene is supported by a solid column of polymer resist. The technology presented in this paper is also applicable for the production of suspended (carbon) nanotube/nanowire devices (with top gates), suspended submicrometer thin anorganic membranes, and electrodes on a polydimethylglutarimide organic dielectric.

V. METHODS

Highly n-doped (0.007 Ωcm) 4 inch Si wafers covered with a 300 nm (or 500 nm) silicon oxide dielectric are used as starting material. Standard optical lithography is used to produce gold markers on the SiO_2 surface, which, in a later stage, will help to locate the dispersed graphene layers on the polymer layer. We spin coat a 1150 nm thick LOR-A layer and bake it on a hot plate at 200 °C for 15 min. This thickness yields good visibility of the graphene in the green

spectrum using an optical microscope. We deposit graphene (HOPG grade YZA) on the polymer using the Scotch tape technique [Fig. 1(a)].² Electron beam lithography is used to fabricate a graphene electronic device. In order to achieve a good undercut for successful lift-off of the EBL patterned structures, we first spin coat a 300 nm thick 50 K molecular weight polymethylmethacrylate (PMMA) layer (AllResist), which we bake on a hot plate at 180 °C for 90 s, and afterward we spin coat a 150 nm thick 450 K PMMA layer (Elvacite 2041 in oxylene) and bake it on a hot plate for 90 s at 180 °C [Fig. 1(b)]. Note that the molecular weight of the PMMA and the type of solvent are not important. The main requirements are that the top PMMA layer has a higher molecular weight with respect to the bottom PMMA layer and that both PMMA resists can be dissolved in hot xylene for the lift-off process. The EBL exposure is done at 30 keV with an area dose of 180 $\mu\text{C}/\text{cm}^2$, and we develop the structures in xylene for 4 min at 21 °C. We have chosen xylene because it does not develop the EBL exposed LOR. After development, we rinse the sample in hexane and blow it dry with nitrogen [Fig. 1(c)]. We evaporate 5 nm of Ti as an adhesion layer and 75 nm of Au using an e-gun evaporator at a pressure of 4.0×10^{-7} mbar [Fig. 1(d)]. A crucial step is lift-off [Fig. 1(e)], which is done in hot xylene (80 °C), an organic solvent that at this temperature is active enough to dissolve the PMMA layers but which does not at all affect the (EBL exposed) LOR. Note that the LOR stays in the solid phase during lift-off because its glass transition temperature (190 °C) is well above 80 °C. After lift-off, we rinse the sample for 60 s in ethylacetate at 21 °C and for 30 s in hexane (21 °C), and we blow it dry with nitrogen. (Note that at a later stage we optimized the lift-off in order to reduce the PMMA polymer remains on the LOR. For this, we blew the sample dry with nitrogen immediately after removing it from hot xylene.) To make the graphene suspended, a second EBL step is used to expose (area dose 1050 $\mu\text{C}/\text{cm}^2$) the LOR underneath the graphene layer [Figs. 1(f) and 1(g)]. We develop in ethylacetate at 21 °C for 60 s to remove the EBL exposed LOR, rinse the sample in hexane, and blow it dry gently with nitrogen. Ultrasonic wire bonding is used to electrically contact the devices. To ensure good ohmic contact between the bonding wire and the contact material (Ti/Au), we introduce a silver paste droplet (dissolved in xylene) at the contact area.

To etch the Hall bar in Fig. 4(a), we introduce two extra fabrication steps in between steps e and f (Fig. 1). We spin coat ~ 100 nm PMMA 400 K dissolved in oxylene on the sample, bake it on a hot plate at 180 °C, expose the parts of the graphene that have to be etched away with 30 keV electrons (dose 180 $\mu\text{C}/\text{cm}^2$), and develop for 4 min in xylene. The Hall bar structure is etched using oxygen plasma in a reactive ion etching system.

ACKNOWLEDGMENTS

We would like to thank Bernard Wolfs, Siemon Bakker, and Johan G. Holstein for technical assistance. This work is part of the research program of the Foundation for Fundamental Research on Matter (FOM) and is supported by NanoNed, NWO, and the Zernike Institute for Advanced Materials.

- ¹Y. B. Zhang, Y. W. Tan, H. L. Stormer, and P. Kim, *Nature* **438**, 201 (2005).
- ²K. S. Novoselov, A. K. Geim, S. V. Morozov, D. Jiang, M. I. Katsnelson, I. V. Grigorieva, S. V. Dubonos, and A. A. Firsov, *Nature* **438**, 197 (2005).
- ³K. I. Bolotin, F. Ghahari, M. D. Shulman, H. L. Stormer, and P. Kim, *Nature* **462**, 196 (2009).
- ⁴X. Du, I. Skachko, F. Duerr, A. Luican, and E. Y. Andrei, *Nature* **462**, 192 (2009).
- ⁵K. I. Bolotin, K. J. Sikes, Z. Jiang, M. Klima, G. Fudenberg, J. Hone, P. Kim, and H. L. Stormer, *Solid State Commun.* **146**, 351 (2008).
- ⁶K. I. Bolotin, K. J. Sikes, J. Hone, H. L. Stormer, and P. Kim, *Phys. Rev. Lett.* **101**, 096802 (2008).
- ⁷X. Du, I. Skachko, A. Barker, and E. Y. Andrei, *Nat. Nanotechnol.* **3**, 491 (2008).
- ⁸K. R. Williams, K. Gupta, and M. Wasilik, *J. Microelectromech. Syst.* **12**, 761 (2003).
- ⁹N. Tombros, C. Jozsa, M. Popinciuc, H. T. Jonkman, and B. J. van Wees, *Nature* **448**, 571 (2007).
- ¹⁰H. B. Heersche, P. Jarillo-Herrero, J. B. Oostinga, L. M. K. Vandersypen, and A. F. Morpurgo, *Nature* **446**, 56 (2007).
- ¹¹G. T. Kim, G. Gu, U. Waizmann, and S. Roth, *Appl. Phys. Lett.* **80**, 1815 (2002).
- ¹²Y. C. Zhao, L. Song, K. Deng, Z. Liu, Z. X. Zhang, Y. L. Yang, C. Wang, H. F. Yang, A. Z. Jin, Q. Luo, C. Z. Gu, S. S. Xie, and L. F. Sun, *Adv. Mater.* **20**, 1772 (2008).
- ¹³K. Yoshimoto, M. P. Stoykovich, H. B. Cao, J. J. de Pablo, P. F. Nealey, and W. J. Drugan, *J. Appl. Phys.* **96**, 1857 (2004).
- ¹⁴C. Lee, X. Wei, J. W. Kysar, and J. Hone, *Science* **321**, 385 (2008).
- ¹⁵J. Moser, J. A. Barreiro, and A. Bachtold, *Appl. Phys. Lett.* **91**, 163513 (2007).
- ¹⁶N. Tombros, A. Veligura, J. Junesch, J. J. van den Berg, P. J. Zomer, M. Wojtaszek, I. J. Vera Marun, H. T. Jonkman, and B. J. van Wees (unpublished).